Earthquake Engineering, Tenth World Conference © 1992 Balkema, Rotterdam. ISBN 90 5410 060 5

Seismic performance of precast concrete columns with lapping joints under shear forces

H. Imai & T. Kobayashi
University of Tsukuba, Ibaraki, Japan

T. Yamaguchi
Kabuki Construction Co., Ltd, Tokyo, Japan

ABSTRACT: A new concept for jointing the main bars of precast concrete columns is proposed. One monolithic column and seven precast columns with and without main bar joints were subjected to constant axial loads and cyclic shear forces. The test results show that the structural performance of the precast columns with and without main bar joints is similar to that of the monolithic column with identical reinforcement.

1 INTRODUCTION

In a frame-type structure with precast members, the locations and methods of jointing the main bars and the concrete give a large influence on the seismic behavior of the whole structure. There has been an abundant production of precast beams and columns which are designed to be connected at the beam-column joints, yet some problems on rebar joints are still left unsolved. It is because of the large design stresses of rebars that the precast member ends have when the main bars are anchored or connected at the abovementioned joints.

In view of this problem, a new concept of jointing method for the frame-type structures using precast members has been proposed. In this concept, the concrete joints are at the member ends, and the connections for rebars are located at the middle of the precast members where the design stresses are small.

The main objective of this paper is to investigate the structural performance of precast concrete columns with lapping joints at mid-height and subjected to shear forces.

2 SPECIMENS

The outlines of column specimens are shown in Fig. 1 and in Table 1. The cross section of each of the columns is 60 cm x 60 cm. This is 60 to 80 percent of the size of the first storey-columns in a 10 to 12 storey-buildings in Japan. The clear height is designed at 120 cm so that a failure in shear will occur before a flexural yielding.

At first, the bar cages of spiral steel sheaths, hoops and lapping bars were assembled. The closed welded rectangular hoops tied the sheaths and the two lapping bars positioned at the opposite sides of each spiral sheath. Next, the concrete was cast. After the curing, each precast column was lifted to a position in such a way that the main bars protruding from the lower beam coincide with the corresponding spiral steel sheaths mounted inside the column. By lowering the column, these bars were inserted into the sheaths through its bottom, afterwhich, the column was set on the lower beam with fresh high strength mortar on the surface. Then, the upper part of the main bars were inserted down into the sheaths from the top of the column. Allowing this mortar to harden for one day to seal some openings in the beam-column joint, the same kind of mortar was pumped in from the bottom of the column to grout the unoccupied space inside the spiral sheaths. Finally, the joint between the partially precast upper beam and the column was cast with an ordinary concrete.

Eight column specimens were made. These were: Specimen RC21, an ordinary monolithic concrete cast vertically, which will be called RC column hereafter; Specimen PC22, a precast column without main bar joints; and six precast columns having main bar joints, with designations PC23 to PC28. All these precast columns are termed PCa columns hereafter. In these six precast columns, there was a variation in the applied axial loads and in the lateral reinforcement of each specimen. This can be seen in Table 1.

The total cross sectional area of the two lapping bars was slightly larger than that of the main bar. With the lapped length being 30 times the lapping bar diameter,

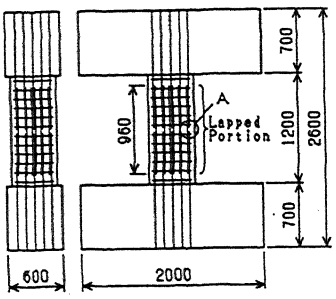

(a) outline

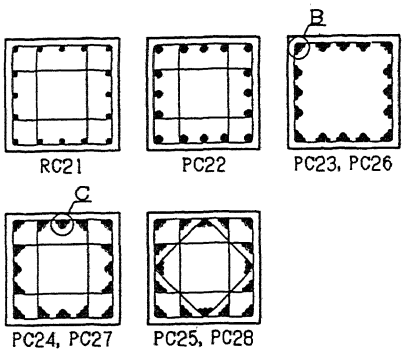

(b) section

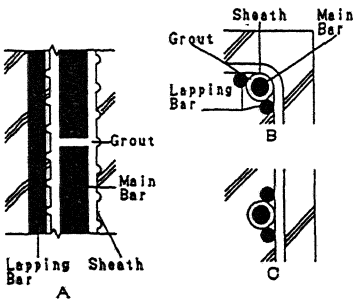

(c) details

Figure 1. Specimens.

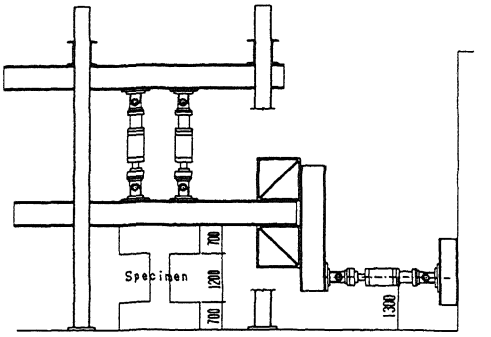

(a) loading apparatus

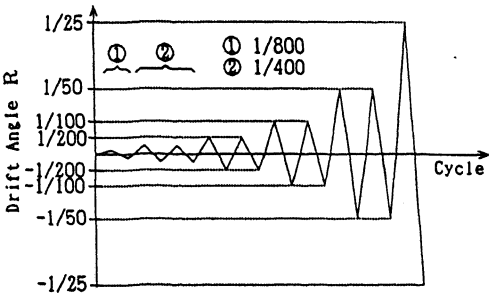

(b) loading history

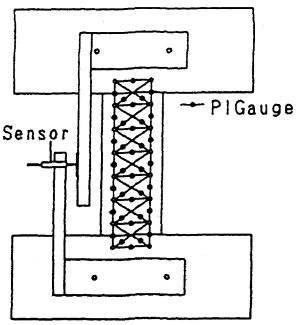

(c) arrangement of sensors

Figure 2. Test Method.

Table 1. Differences among specimens.

Specimen	Concrete	Rebar Joint	Shear Rein.	Axial Load (kgf/sq. cm)
RC21	Monolithic	none	4-D10 @100	
PC22				
PC23		Lapping	2-D10 @100	30
PC24		Bars for	4-D10 @100	
PC25	Precast	each Main	4+√2-D10 @100*	
PC26		Bar	2-D10 @100	
PC27		2-D16	4-D10 @100	60
PC28		(SD345)	4+√2-D10 @100*	

Common
b × D : 50 cm × 50 cm
h : 120 cm
Main Bar : 16-D22 SD345
Concrete : Fc300
Sheath : Diameter 34 mm
Lug Height 2 mm
Pitch 28 mm

*√2 in Shear Reinforcement denotes diagonal hoops

the length of each lapping bar is 60 times that diameter.

3 TEST METHOD

Each column specimen was subjected to shear forces which produced anti-symmetric bending moments while being acted upon by a constant axial load. (N/BD=30 or 60 kgf/sq. cm) as shown in Fig. 2(a). The varying shear force applied continuously in a cyclic manner caused the specimens to drift twice at drift angles R=1/400, 1/200, 1/100 and 1/50 and once at R = 1/25 as shown in Fig. 2(b).

Throughout the loading process, the relative horizontal displacements between the upper and the lower beams were measured on both sides of each column using displacement sensor holders fixed at both beams as shown in Fig. 2(c). The local deformations at different points were determined using clip type sensors, the locations of which are also shown in Fig. 2(c). The strains of the rebars were also measured.

4 TEST RESULTS OF MATERIALS

The results obtained from testing both the rebars and the concrete are given in Table 2. The compressive strength of concrete and of grouted mortar are at about 300 kgf/sq. cm and 700 kgf/sq. cm, respectively. The yield stresses of reinforcing bars are 10 to 20% higher than the specified ones.

5 TEST RESULTS AND DISCUSSIONS

5. 1 Crack patterns

Crack initiation due to bending took place at the top and bottom ends of each column when the drift angle R was 1/800. When R = 1/400 there were crack propagations which were mainly due to continuous bending on the initially damaged portion. Also at this stage, initial shear cracks were observed, although in some specimens, these cracks were still submicroscopic. When the drift angle R reached 1/200, the shear crack growth became rampant as could be seen on the surface of all the specimens. Diagonal cracks from corner to corner were observed on PC23 and PC26, the specimens with a small amount of outer hoop reinforcement.

It was observed that the crack patterns which occured on the RC column without rebar joints, and on the PCa columns with or without reinforcement joints, appeared to be similar even though there was a variation in the magnitude of the applied axial load. Typical crack patterns when R = 1/400 and R = 1/100 are shown in Fig. 3.

When R = 1/50, there were more fine cracks on the RC column compared to the PCa columns. The cracks grew deep enough producing stress concentrations exceeding the bond strength and eventually caused bond failure. This happened to Specimens PC23 and PC26 when R was 1/25. In PC25,

Table 2. Properties of materials.

(a) rebars.

(kgf/cm^2)

Specimen	RC21		PC22～28		Grout
	Comp.	Split	Comp.	Split	Comp.
Specified	300	–	300	–	600
28 Days	296	–	295	25. 8	691
Actual(Exp.)		18. 6	300	25. 0	778

(b) concrete

(kgf/mm^2)

size	Grade	Young's Modulus (x10^4)	Yield Stress	Tensile Strength	Elongation (%)	Remarks
D22	SD345	2. 14	39. 7	58. 0	15. 6	Main
D16	SD345	1. 81	37. 7	57. 0	18. 2	Loapping
D10	SD295	1. 91	38. 0	51. 3	19. 5	Hoop

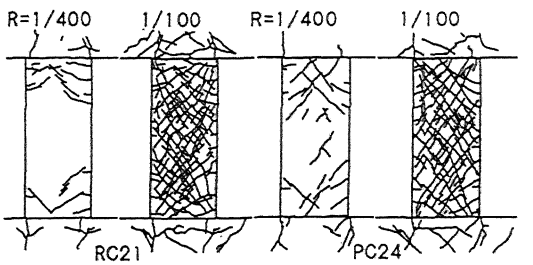

Figure 3. Crack patterns.

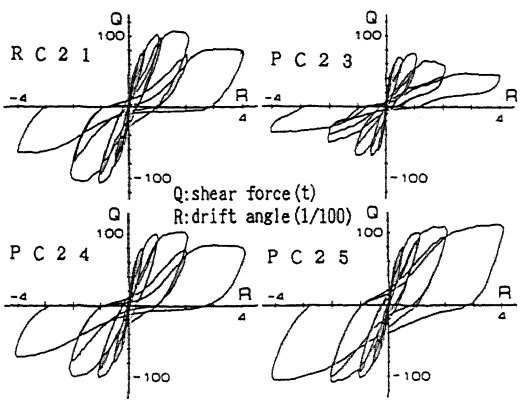

Figure 4. Shear - drift angle curves.

where all the main bars were confined laterally by shear reinforcement, the shear cracks propagated, but the crack openings remained small. On the other hand, excessive shear cracks caused the other specimens to fail in shear.

5. 2 Load - displacement relationships

The curves for the shear force versus the horizontal drift angle (Q-R curves) are shown in Fig. 4. In the diagrams, the features of a bond failure in PC23, a flexural yielding in PC25, and a shear failure in the other specimens can be observed.

The envelope curves of the shear force - drift angle relationships are shown in Fig. 5. It can be noticed that there is no much difference between the envelope curves of the RC column and those of the PCa columns. The same is true if the columns with rebar joints are compared with those without reinforcement joints.

Specimen PC27, the column which was subjected to a larger axial load, showed a higher shear strength capacity compared to PC24, the specimen which was loaded with a smaller axial force, but, after the maximum load, the reduction of the horizontal carrying capacity of the former was more severe than that of the latter. The specimen which has more shear reinforcement proved to be more ductile and stronger in resisting shear stresses.

5. 3 Partial deformation

The curvature and shear distortion distribution diagrams are shown in Fig. 6. The diagrams for the curvatures are almost similar to those of the bending moment distributions. Shear distortions are large at the middle of the columns. No difference was noticed between RC and PCa columns regarding this matter.

Each deformation due to bending and due to shear is calculated from the abovementioned curvatures and shear distortions, respectively. In each specimen, the sum of these two deformations was almost similar to the relative displacement recorded in the displacement sensor holders.

The partial deformation total deformation ratios for bending and shear are shown in Fig. 7. It can be observed that there is no large difference between the results of RC column and those of the PCa columns even with or without main bar joints and subjected to different axial forces.

When the driftage is small, in specimens with the same shear reinforcement, the ratios of flexural deformation to total

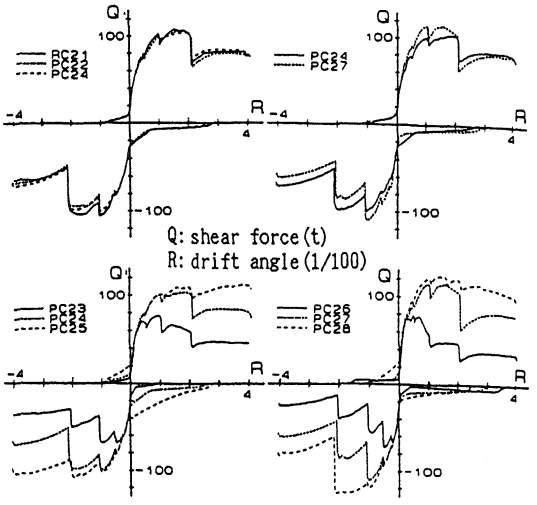

Figure 5. Shear - drift angle curves.

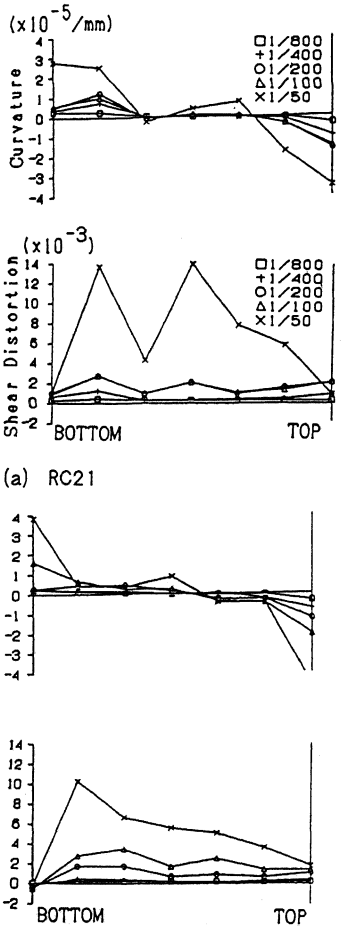

(a) RC21

(b) PC24

Figure 6. Distributions of curvatures and shear distortions.

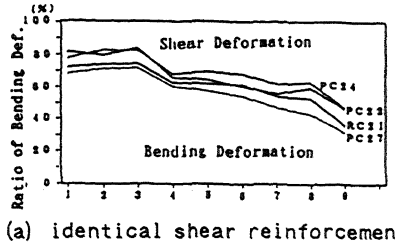

(a) identical shear reinforcement

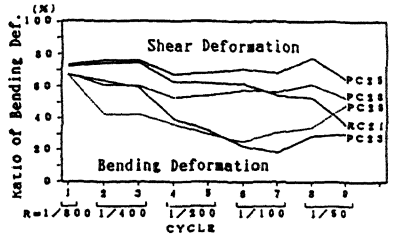

(b) different shear reinforcements

Figure 7. Components of bending and shear deformations.

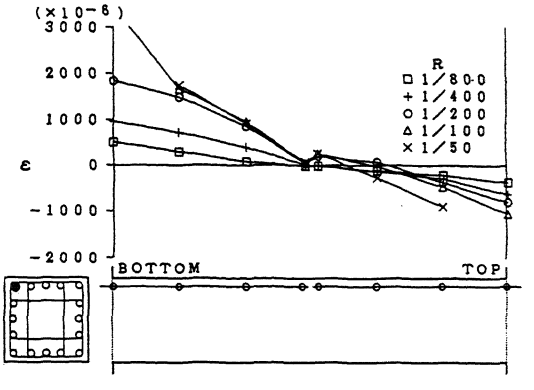

(a) longitudinal distribution

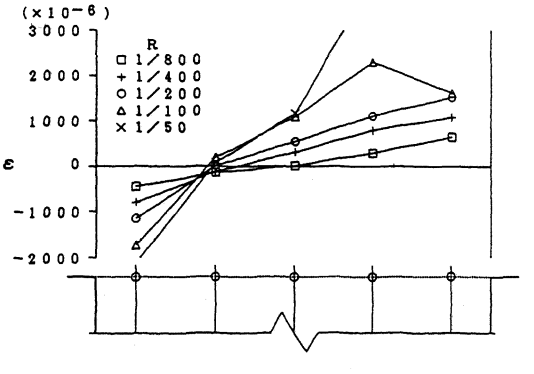

(b) distribution at the top section

Figure 8. Strain distributions of main bars

displacement range from 0.7 to 0.8, but the shear deformation gradually becomes larger.

Finally, after large driftage, the percentage of flexural to total deformation drops to a range of 30 to 40 percent.

PC23 and PC26, the specimens without inner shear reinforcement show similar characteristics when compared to other specimens, but, the proportions of shear deformation gradually increase to about 80% of the total deformation at R=1/100. PC25 and PC28, the columns with the largest amount of shear reinforcement, exhibit the same features as the other columns until R=1/200, but their ratios of shear deformations remain almost constant until R=1/50.

5.4 Distribution of bar strains

A sample of strain distributions in the longitudinal bar at the corner of the column section is shown in Fig. 8(a). It is similar to that of the bending moment distribution.

The strain distribution on the main bars at the column's bottom cross section is shown in Fig. 8(b). The assumption that a plane section before deformation remains plane after deformation can be observed in the strain distribution of the longitudinal bars at the top and bottom sections of the column.

The main bars of PC23 and PC26, the columns without inner shear reinforcement did not yield. The outer main bars of PC25, the one with the heaviest shear reinforcement and loaded with a comparatively small axial force yielded at R=1/100. The outer main bars in other specimens yielded at R=1/100 to R=1/50, but the inner main bars did not yield.

A typical strain distribution diagram of lapping bars can be seen in Fig. 9. These bars behaved elastically until R=1/100, but at large deformation, local yielding due to shear cracks occurred on them.

The strain distribution diagrams of shear reiforcements are shown in Fig. 10. The outer hoops, which were positioned in the loading direction, yielded at R=1/50 in RC and PCa columns except PC23 and PC26. The outer hoops of PC23 and PC26, the columns which have no inner hoops, yielded at R = 1/200 to 1/100. In RC21, PC22, PC24, and PC27, the specimens with the same amount of shear reinforcement, the inner hoops in the loading direction yielded at R = 1/100 to 1/50. The differences between the strains of the outer hoops and those of the inner hoops of RC and PCa columns were not large even with or without the main bar joints.

The hoops of PC27 under large axial force yielded more severely compared to those of the other columns. The inner and the diagonal hoops of PC25 and PC28, the

specimens which were heavily reinforced in shear, also yielded, but the maximum values were only within the range 3000 to 4000 micro.

5.5 Shear strength

The experimental and the calculated shear strength values are listed in Table 3 and graphed in Fig. 11. For all the specimens, the calculated values, which were obtained using Dr. Arakawa's equation, are considerably lower. The calculated shear strength values, based on the Arch and Truss Model theory in the ultimate strength design guidelines specified by the Architectural Institute of Japan (AIJ), agree well with the actual test results both for RC and PCa columns. Much closer value can be obtained if a factor, 0.1 multiplied by the constant axial stress, is added to either the value obtained using method A of the Arch and Truss Model theory or the one using Method B, whichever is smaller. This factor can be regarded as an effect due to axial force.

5.6 Hysteresis energy absorption capacity

The ratios of the absorbed hysteresis energy of each specimen to that of RC21 are shown

Table 3. Shear strengths.

Specimen	Calculated (ton)			Experimental (ton)	Experimental÷Calculated		
	Arakawa Eq.	Final Strength Method			Arakawa Eq.	Final Strength Method	
		A Method	B Method			A Method	B Method
RC21	70.4	100.6	96.1	108.1	1.54	1.07	1.12
PC22	70.2	100.4	96.1	105.3	1.50	1.05	1.10
PC23	62.9	70.5	79.9	76.7	1.22	1.08	0.96
PC24	70.4	100.6	96.1	103.5	1.47	1.03	1.08
PC25	74.6	121.8	108.0	112.4	1.51	0.92	1.04
PC26	69.1	71.0	79.9	79.1	1.14	1.11	0.99
PC27	76.5	100.8	96.1	115.2	1.51	1.14	1.20
PC28	80.6	121.8	108.0	123.1	1.53	1.01	1.14

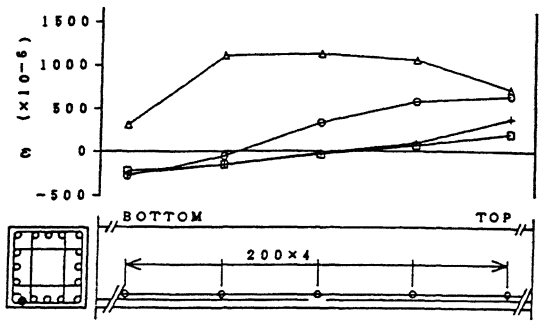

Figure 9. Strain distribution of a lapping bar.

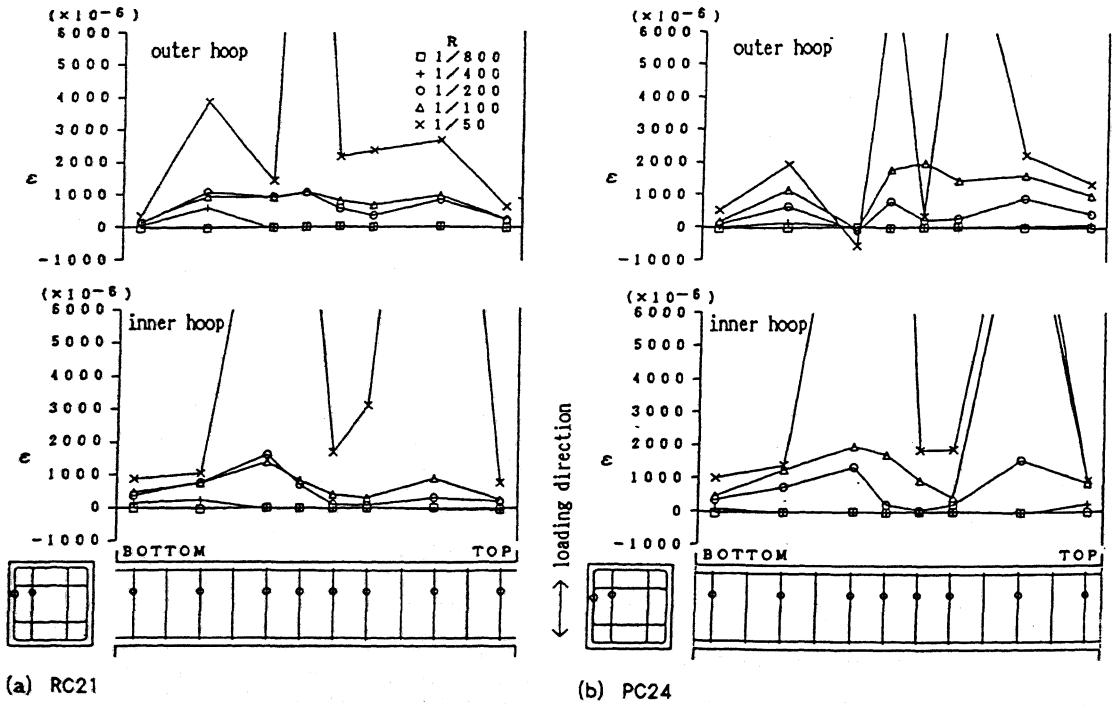

Figure 10. Strain distributions of shear reinforcements.

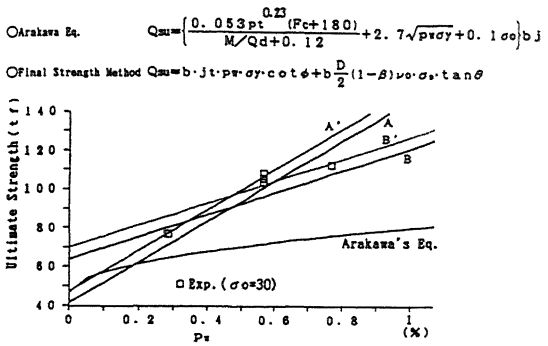

Figure 11. Relationship between shear strength and shear reinforcement ratio.

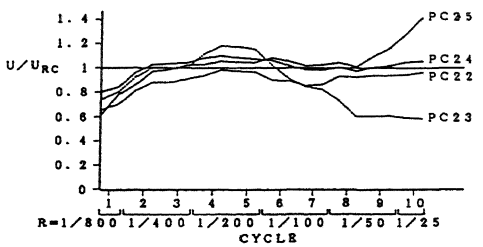

Figure 12. Hysteresis energy.

Fig. 12. At R = 1/800, the hysteresis energy of each of the PC columns is about 80% of that of the RC21. At R = 1/400 to R = 1/100, these are almost the same inspite of having main bar joints. After R=1/400, specimens which have shear reiforcement similar to that of RC21 give the same energy absorption capacity. The effect of shear reinforcement was noticed only when R=1/50. At the final stage, when R=1/25, PC23, the column without inner hoops, has only about 60% of energy absorption capacity of RC21, while PC25, the one with inner and diagonal hoops, attain 140% of the abovementioned energy.

6 CONCLUSIONS

From the foregoing dicussions, the following conclusions were obtained:

1) The performance of a precast concrete column with lapping joints, considering the crack patterns, shear strength, and deformation capacity, is similar to that of the monolithic column with identical reinforcement.

2) The inner hoops are effective in preventing bond failure at the outer surface of the spiral steel sheaths.

3) The shear strength of a precast column with main rebar joints at the mid-height can be calculated using the Arch and Truss Model analytic theory specified by the AIJ.

REFERENCES

Castro, J. J., Yamaguchi, T. & Imai, H. 1992. Seismic performance of precast concrete beam column joints. 10WCEE

Yanez, R., Yamaguchi, T. & Imai, H. 1992. Bond performance of a lapping joint developed for precast concrete columns. 10WCEE